iScience

CellPress
OPEN ACCESS

Article

Microplastic and adhesive free, multifunctional, circular economy approach-based biomass-derived drinking straws

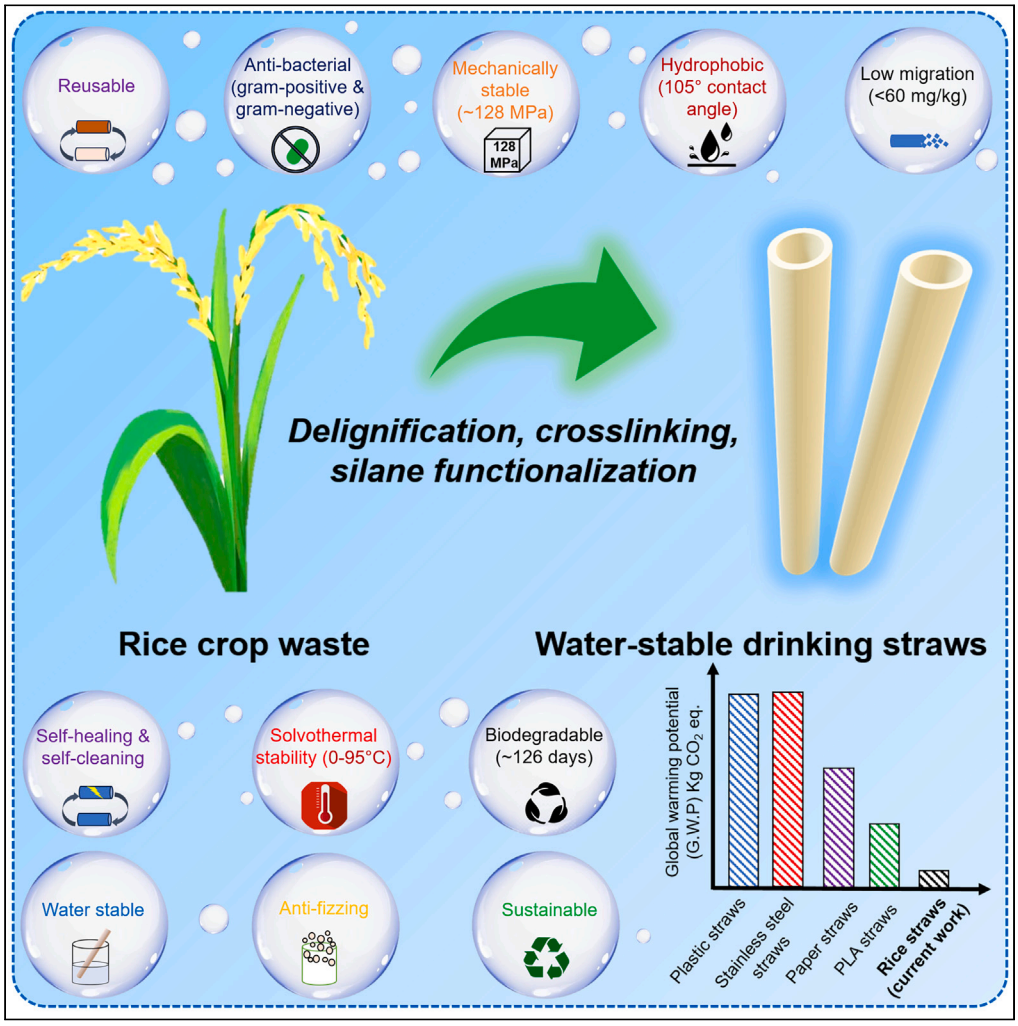

Rohit Rai, Rahul Ranjan, Chandra Kant, Prodyut Dhar

prodyut.bce@iitbhu.ac.in

Highlights

Utilization of rice waste for fabrication of cellulose-silica-based biodegradable straws

Hydrophobic straws with high water stability, mechanical strength, and low leaching

Straws with antibacterial, self-cleaning, self-healing and reusable features

Functional, sustainable straws with lower carbon footprints than metal and PLA straws

Rai et al., iScience 27, 109630
May 17, 2024
https://doi.org/10.1016/j.isci.2024.109630

iScience

CellPress
OPEN ACCESS

Article

Microplastic and adhesive free, multifunctional, circular economy approach-based biomass-derived drinking straws

Rohit Rai,[1] Rahul Ranjan,[1] Chandra Kant,[2] and Prodyut Dhar[1,3,*]

SUMMARY

Generation of voluminous single-use plastic waste and byproducts from agricultural harvests such as rice straws (RSs) are major global challenges due to their disposal issues, contributing to greenhouse gas emissions, and affecting the ecological system with threats to human health. A scalable, low-cost, and eco-friendly strategy for fabricating cellulose-silica-based drinking straws, free from microplastics and adhesive, through strategic valorization of RS is reported. Functionalization by delignification-*cum*-crosslinking of RS leads to development of straws with high water stability (~5 days), solvothermal stability (0°C–95°C), tensile strength (128 MPa), low migration values (<60 mg/kg), improved biodegradability (~126 days) with reduced wettability and hydrophobicity. RS drinking straws show antibacterial, self-cleaning, self-healing, anti-fizzing, reusable, and generate significantly lower carbon footprint (<99.8% and <53.34% global warming potential than metal and polylactic acid straws). Repurposing of agro-wastes from farms to commercially viable drinking straws which biodegrades after its consumption achieves the goal of circular economy and sustainable development.

INTRODUCTION

Rice is one of the most produced and consumed crops, feeding more than 40% population worldwide. The production of rice has risen from ~600 million tons in 2000 to ~787 million tons in 2021 globally which suggests its capacity to generate large amounts of waste lignocellulosic biomass.[1] Asia is solely responsible for over 90% of global rice production which also leads to the generation and accumulation of agro-wastes in the form of straws and husks.[2] The lack of strategies for the up-conversion of rice agro-waste into commercially viable products makes disposal of rice crop waste a major challenge due to which it is either left for landfilling or burned uncontrollably.[3] Stubble burning is a major issue in South-Asian countries with India itself contributing to 13% of global emissions, of which ~60% originates from burning rice straw (RS) generating harmful greenhouse gas emissions such as nitrogen oxides (NO_x), methane (CH_4), carbon monoxides (CO), carcinogenic polycyclic aromatic hydrocarbons (PAH) along with smoke and soot.[4] These lead to severe environmental damage along with health disorders that forms a part of the major global challenges faced today; therefore, novel strategies to develop value-added products utilizing RS is need of the hour.[5] RS is majorly composed of cellulose (34–40%), hemicellulose (20–28%), lignin (12–14%), and silica (9–14%), all of which have interesting physio-chemical properties with potential for value-added applications.[6] The silica present in RS is polymerized in the epidermal cell wall containing cellulose, forming silica double layers under cuticle, which can be extracted through strategic delignification and functionalization approaches.[7] Recently, RS has been used for various applications including bioadsorbent,[8] soil enrichment,[9] concrete additives,[10] sensors,[11] food packaging,[12] biochar,[13] and biofuels,[14] which opens up new avenues for the valorization of rice waste to high-performance materials.[15,16]

In the 21st century, the vast consumption of non-degradable plastics for packaging has led to tremendous pollution in aquatic, terrestrial, and atmospheric ecosystems; however, the use of plastics is still prevalent because of its durability, low cost, easy processability, and scalability. About 300 million tons of single-use or reusable plastics are produced every year and consumed in the form of plates, spoons, and straws.[17] Due to their non-degradable nature, biological and chemical resistance, poor recyclability, and short-use cycle, plastic straws accumulate in the environment for several decades, threatening human health.[18] The emergence of microplastics (<5 mm size) and their contamination with food products like drinking water, table salt, etc. is a major concern that may lead to fetal growth restriction and detrimental growth effects with developmental abnormalities in plants and animals.[19,20] Paper straws can replace plastics; however, poor mechanical properties, and high swelling which require utilization of adhesives/wax coatings hamper its biodegradability with the generation of fizz in beverages, making them undesirable for long-run applications. Biopolymers like chitin, polylactic acid (PLA), and abundantly available agricultural lignocellulosic biomass due to their improved properties, biodegradability, and low toxicity, can be a potential alternative to

[1]School of Biochemical Engineering, Indian Institute of Technology (BHU), Varanasi 221005, Uttar Pradesh, India
[2]Department of Chemical Engineering and Technology, Indian Institute of Technology (BHU), Varanasi 221005, Uttar Pradesh, India
[3]Lead contact
*Correspondence: prodyut.bce@iitbhu.ac.in
https://doi.org/10.1016/j.isci.2024.109630

plastics.[21,22] Dong et al.[23] prepared mechanically strong, biodegradable, and water-stable drinking straws using lignocellulosic biomass with flexural strength ~62 MPa, tensile strength ~127 MPa, and hydrostability for ~150 days. Wang et al.[24] interestingly utilized cellulose nanofiber and microfiber hybrids to fabricate binder-free mechanically strong (tensile strength ~70 MPa), biodegradable, hydrostable, low-cost drinking straws. In another study, Wang et al.[25] utilized cellulose-lignin reinforced composites for the drinking straws fabrication with high stiffness (2.8 GPa), water stability (4 h), biodegradability (~100 days), and reduced wettability (contact angle ~120°). Yang et al.[22] fabricated drinking straws using biosynthesized bacterial cellulose and alginate coating showing high mechanical strength (~420.5 MPa), biodegradability (~45 days), and water stability. Chen et al.[21] used chitin for making straws with high mechanical strength (flexural strength ~19.7 MPa), improved biodegradability (~100 days), and water stability. Rai et al.[26,27] recently processed delignified bamboo for fabrication of water-stable (~16–24 h), biodegradable (36–98 days), and mechanically strong drinking straws with reduced wettability (~87.8°–103.3°). Despite the impressive properties of biopolymers, multiple chemical modification steps are required to improve its wettability and strength, which adds to the cost, making it difficult to translate at a commercial scale. The contribution of chemical processing to the cost for making drinking straws from biomass can be minimized by selecting waste biomass substrates that require minimal processing for fabrication of beverage stable straws. One such alternative is RS waste which due to its lignocellulosic composition and high silica content is inherently water-stable with reduced wettability and has not been reported for utilization as drinking straws till date.

A facile, scalable, and eco-friendly strategy for the fabrication of perfectly rolled, flexible, biodegradable drinking straws from RS with high water stability, self-cleaning, self-healing, anti-fizzing, reusable, and antibacterial properties is proposed. Two different forms of RS, firstly, naturally closed culm was directly delignified, whereas open, rolled leaf sheath was delignified followed by crosslinking open ends with citric acid (CA) for the fabrication of drinkable straws. The delignification-*cum*-crosslinking of RS improves tensile, flexural strength, wettability, and water stability, making it suitable for drinking straw applications. The straws were strategically functionalized with curcumin and (3-aminopropyl)triethoxysilane (APTES) for the incorporation of antibacterial and self-cleaning properties. The drinking straws are in direct contact with food, therefore, solvothermal stability (0°C–95°C) and migration studies were carried out using different food simulants such that it is within the prescribed limits (<60 mg/kg). The assessment of biodegradability and environmental sustainability of developed straws were studied through life cycle analysis (LCA) and compared with other commercially available straw alternatives. RS straw produced in the current study is cellulose-silica based, adhesive-free, cost-effective with easy scalability, and a sustainable alternative to commercially used single-use paper and plastic-based straws.

RESULTS AND DISCUSSION

Methods summary

Rice, as one of the most cultivated crops globally generates a large quantity of lignocellulosic straw waste which has been converted into smart drinking straws with interesting functional properties. The harvested rice plants contain flexible culms in stems (9.6 cm–83.6 cm length range) that are naturally rolled and separated by closed internodes. The culms portion of rice stem is covered by a rolled but open leaf sheath which can be expanded-like a sheet. The present study reports the preparation of RS-based drinking straws using both naturally rolled closed culms, as well as opened leaf sheath portions. The culm and leaf sheath were separated from RS by making an incision between the nodes. The culms and leaf sheath were then delignified following single-step treatment with sodium chlorite and the open stem portions were cross-linked to join the ends of delignified leaf sheath (Figure 1). Delignification was carried out using dilute sodium chlorite treatment which is a fast, efficient, reproducible, cheap, and low chemical consuming method for large-scale straw production. It selectively removes the lignin present in RS and preserves the inherent cellulose-silica structure, required for the formation of straws with high mechanical strength.[28–30] The cellulose-silica composites from delignified RS culms are denoted as DRS whereas delignified open leaf sheath portions, cross-linked with CA, were named as opened delignified RS (ODRS_CA). Modification with a silane coupling agent and curcumin was also performed with DRS to equip it with self-cleaning, reusable, and antibacterial properties. Both DRS and ODRS straws were subsequently characterized to evaluate their physiochemical, structural properties, and process sustainability using LCA followed by assessing straw features to determine their potential to replace single-use plastic/paper-based straws.

Physiochemical properties of delignified and cross-linked RS

The DRS and ODRS straws were analyzed for changes in crystal properties post-chemical modifications using X-Ray diffraction (XRD) (Figure 2A). RS shows two peaks at 15.8° and 22° corresponding to lattice planes (110) and (200), with C.I of 37.4%, and %crystallinity of 41.6%. The distinctive peaks of cellulose in DRS remain unchanged; however, C.I and %crystallinity increased to 44.4% and 50.7%, respectively, on the removal of lignin. Cross-linked ODRS, shows a slight shift in peak from 15.8° to 16.4° due to crosslinking of cellulose with CA during straw preparation; however, no apparent shift in peak at 22° was observed. On cross-linking, improvement in C.I. and %crystallinity was observed for ODRS_1.6CA to ~48.9% and 49.8%, respectively, and in the case of ODRS_3CA to ~50.5% and ~56.3%, respectively.

Fourier-transform infrared (FTIR) analysis was conducted to analyze the change in functional moieties after RS delignification and cross-linking of ODRS for the fabrication of drinking straws. RS and DRS show peaks at 3330 cm^{-1} and 2920 cm^{-1} originating from -OH groups present in cellulose and C-H stretching in hemicellulose and cellulose, respectively (Figure 2B). The peaks at 1735 cm^{-1}, 1635 cm^{-1}, and 1450 cm^{-1} represent C=O, C=C, and C-C bond stretching arising from lignin present in RS, and upon delignification, the intensity of these peaks reduces significantly in DRS. The characteristic peaks for cellulose and hemicellulose were present in DRS at 1170 cm^{-1}, 1030 cm^{-1}, and 940 cm^{-1} representing C-O-C bonds, and C-C bending from cellulose and hemicellulose. The ODRS_1.6CA and ODRS_3CA show an increase in the intensity for C-H bonds at 2920 cm^{-1} and 2855 cm^{-1} from the hydrocarbon backbone of CA used during crosslinking. A

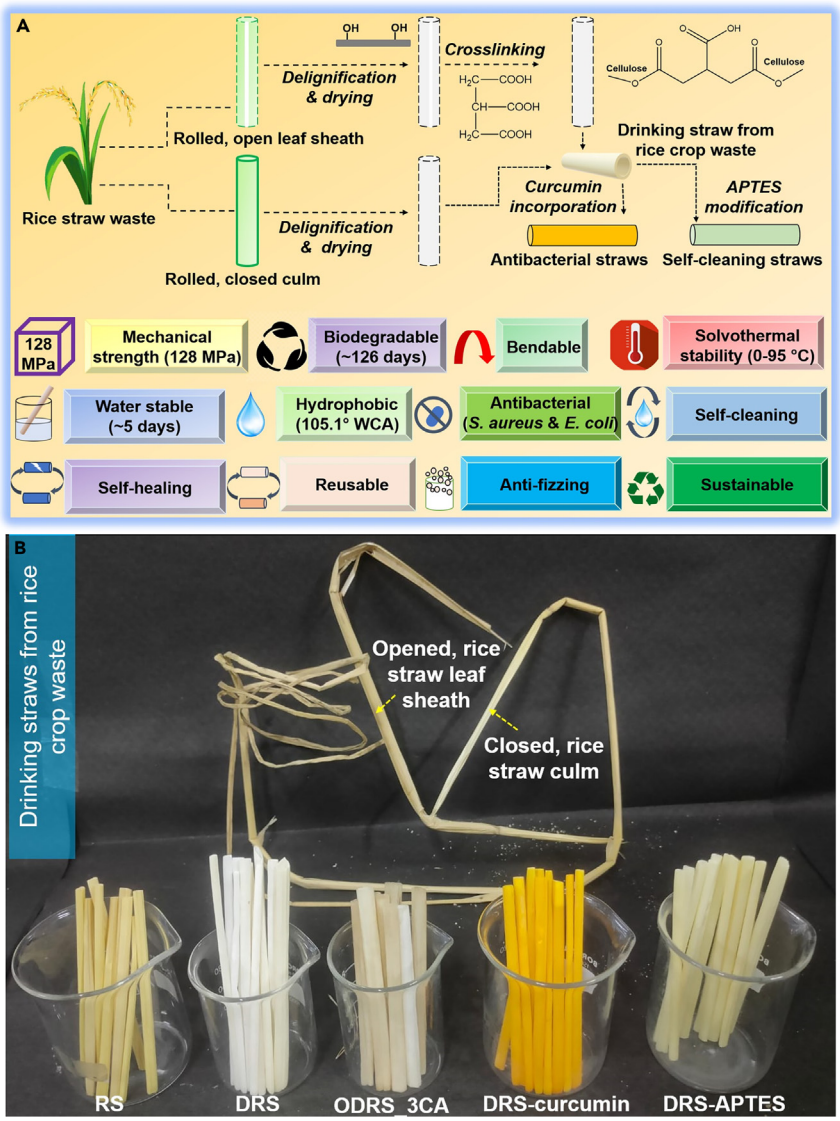

Figure 1. An overview of drinking straw fabrication with rice crop waste

(A) Schematic overview for fabrication of drinking straws from rice biomass waste along with evaluation of their physiochemical, structural, biodegradation, self-cleaning, self-healing, anti-fizzing, washability, antibacterial properties and migration studies required to evaluate their potential for drinking straw applications. (B) RS showing closed straw culms and opened leaf sheath along with varieties of drinking straw samples RS, DRS, ODRS_3CA, DRS- curcumin, and DRS-APTES prepared in this study.

peak at 1710 cm^{-1} was also observed for ODRS_3CA and ODRS_1.6CA suggesting the presence of carboxyl groups of CA. The peak at 1635 cm^{-1} was observed in ODRS_1.6CA and ODRS_3CA which emerges due to crosslinking of hydroxyl groups of cellulose with carboxylic moieties of CA resulting in the joining of open-end delignified portions of rice stem. The peaks at 1170 cm^{-1}, 1030 cm^{-1}, and 940 cm^{-1} represent C-O-C stretching, and bending of C-C from cellulose and hemicellulose in DRS (Table S1). For all the samples, a peak at 785 cm^{-1} was observed which corresponds to Si-O-Si linkages, due to the inherent presence of silica in RS. FTIR confirms the removal of lignin and hemicellulose during the delignification step along with the crosslinking of carboxyl and hydroxyl groups of cellulose with CA, required to prepare straws.

The drinking straws can be subjected to varied temperatures during the consumption of beverages; therefore, an assessment of thermal stability was carried out using thermogravimetric analysis (TGA). Drinking straws ideally should not show disintegration or swell in the presence of hot liquids and should be stable at the temperature range for consumption of hot or cold beverages. RS shows T_{onset}, T_{max}, and percent residual weight of 263°C, 344°C, and 14.4%, whereas DRS shows a slight improvement in T_{onset}, T_{max}, and percent residual weight of 269°C, 343°C, and 15.1%, respectively. ODRS_3CA samples present a T_{onset}, T_{max}, and percent final remaining weight of 207°C, 313°C, and 7%, respectively (Figure 2C). The thermal profile of RS, DRS, and ODRS_3CA straws up to 100°C shows a slight loss in weight by

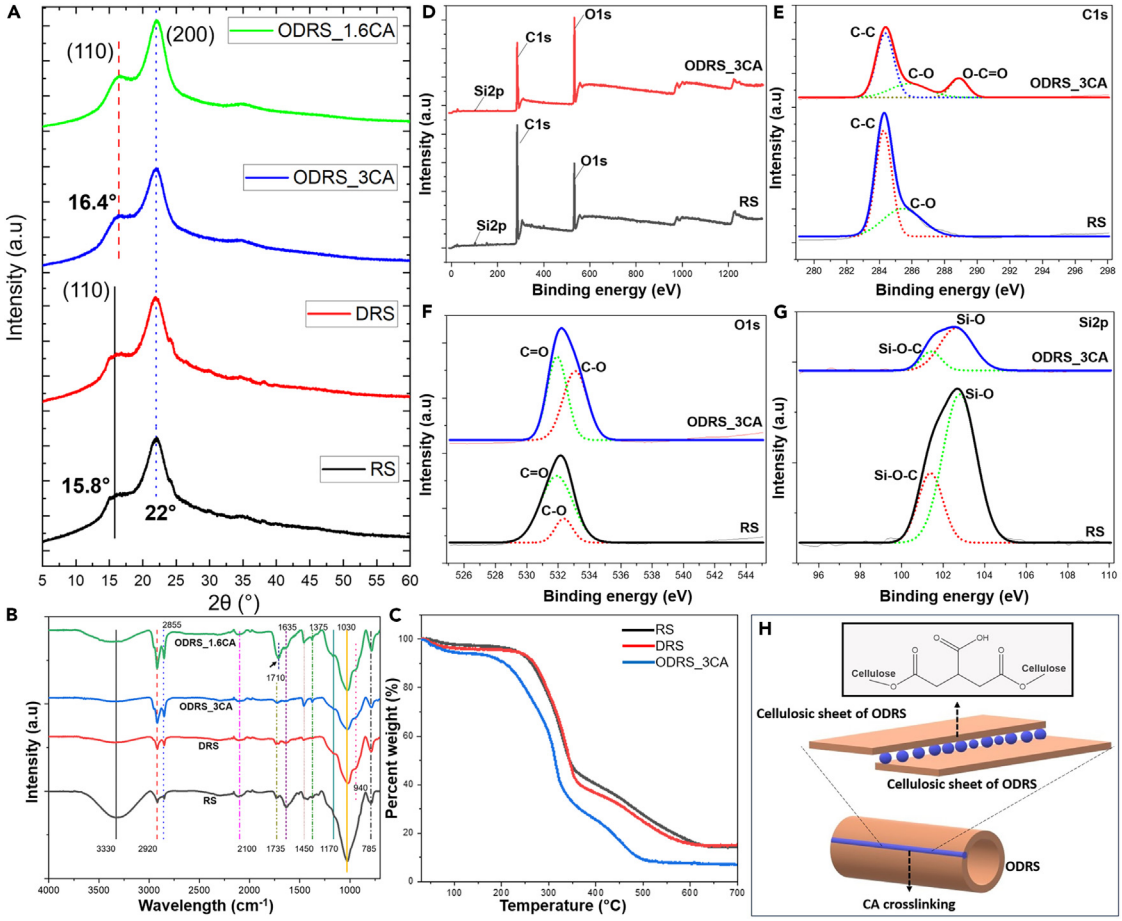

Figure 2. Physiochemical properties of RS, DRS, ODRS_1.6CA, and ODRS_3CA

(A) XRD.

(B) FTIR analysis, also see Table S1.

(C) TGA analysis of RS, DRS, ODRS_3CA, and ODRS_1.6CA samples.

(D) XPS spectra of RS and ODRS_3CA with high-resolution.

(E) C1s spectra.

(F) O1s spectra.

(G) Si2p spectra.

(H) Mechanistic representation of ODRS crosslinking with CA for straw preparation.

2.3%, 3.7%, and 5.5%, respectively, suggesting enhanced stability of rice-based straws for consumption of hot beverages. For RS, major weight loss by ~51.4% occurred between 201°C–360°C which slightly improved to 229°C–360°C in the case of DRS (major weight loss by~53.5%). For ODRS_3CA, an increased weight loss of ~59.4% was observed from 157.5°C–343.2°C, due to depolymerization of cellulosic backbone. From TGA analysis, it was observed that delignification of RS, does not significantly affect the thermal stability of straws; however, ODRS upon crosslinking shows a reduction in thermal properties. This reduction in thermal stability of ODRS_3CA at temperature >150°C is due to the presence of CA in cross-linked straws which initiates the early degradation and catalyzes the rate of thermal degradation profile.

X-ray photoelectron spectroscopy (XPS) was carried out to study the chemical composition of RS and the changes in functionalities during delignification-*cum*-crosslinking step for the preparation of drinking straws. The XPS survey of RS and ODRS_3CA shows peaks for C1s, O1s, and Si2p at 285.08 eV, 532.08 eV, and 102.08 eV, respectively (Figure 2D). The high-resolution spectra of C1s (Figure 2E) show peaks at 284.3 eV and 285.5 eV representing C-C and C-O bonds, respectively, corresponding to lignocellulosic components in RS. The deconvoluted C1s spectra of ODRS_3CA display peaks at 284.3 eV, 286 eV, and 288.9 eV representing C-C, C-O, and O-C=O bonds. The additional O-C=O peak for ODRS_3CA comes from the CA used for crosslinking the ODRS. The high-resolution spectra of O1s show peaks at 531.3 eV representing C=O and 532.4 eV for carbonyl oxygen (O-C) originating from the lignocellulosic backbone of RS (Figure 2F). ODRS_3CA, on the other hand, presented a peak at 531.3 eV for C=O and an intense C-O bond peak at 533.1 eV, respectively. The C=O peaks in ODRS_3CA come from the CA used during crosslinking of ODRS whereas the intense C-O peaks appear due to the crosslinking of hydroxyl groups of cellulose with the carboxyl groups on the CA via C-O linkages (Figure 2H). The crosslinking of ODRS with carboxyl group-rich CA can also be observed

by comparing the C/O ratio of ODRS and RS which presented a reduced value of 2.18 compared to 4.16 (for RS). In high-resolution spectra of Si2p, peaks at 101.4 eV and 102.8 eV represent C-Si-O and Si-O groups found in silica that is bound to lignocellulosic components of RS and ODRS_3CA (Figure 2G). The presence of silica (~2%) in RS is responsible for the hydrophobic properties, required for drinking straws with improved water stability as discussed in the subsequent sections.

Morphological and mechanical characteristics of RS-based drinking straws

Scanning electron microscopy-energy dispersive X-ray spectroscopy (SEM-EDX) was performed to observe the morphological changes that occurred during the delignification and crosslinking of ODRS with CA along with elemental distribution and quantification (Figures 3A–3C). RS shows a rough surface with the presence of pits in the structure along with a uniform distribution of spherical to oval-shaped silica microparticles. DRS also shows a coarse texture with an array of circular-shaped silica (2–5 microspheres per aggregate) with a size distribution of $\sim 1.52 \pm 0.16\ \mu m$. The presence of silica in microparticles was confirmed by EDX and elemental mapping which shows its uniform distribution throughout the surface of RS and DRS (Figures 3D and 3E). EDX analysis also confirmed the presence of silica (44.8–46.7%) in the scanned portion for both RS and DRS, along with C (14.8–16.7%) and O (36.5–40.3%) (Figure S1). As shown in schematic Figures 3G and 3H, the silica microspheres were distributed evenly half embedded onto the surface of cellulose in DRS creating a highly ordered patterned texture. The inherent hydrophobicity of DRS comes from the chemical nature of SiO_2 microspheres along with the patterned surface texture which prevents the seeping or spreading of water droplets onto DRS surface (Figure 3H). Upon crosslinking the open sheets with CA, a smooth surface covering the rough inherent structure of ODRS was observed (Figure 3C). The presence of CA in ODRS_3CA results in a non-uniform patch-like distribution of Si in contrast to the uniform presence in RS and DRS (Figure 3F). The EDX also shows low silica content (21.9%) in the scanned portion along with increased C (31.1%) and O (46.8%) due to the presence of CA. This is due to the overlapping of open ends of straws forming covalent linkages between the hydroxyl groups of cellulose and carboxyl groups of CA, as mechanistically explained in Figure 2H. From SEM-EDX analysis, an interesting micro-pattern of silica distribution is observed along with the cross-linking of open RS sheaths in ODRS.

Evaluating the mechanical properties of drinking straws is necessary to determine the structural stability of straws toward mechanical stress. RS straws show tensile strength of 117 MPa, flexural strength of ~2.73 MPa with tensile and flexural modulus of ~1.95 GPa and 34.1 MPa (Figures 3I and 3K). On delignification, tensile and flexural strength improved to 128 MPa and 2.75 MPa, with tensile and flexural modulus of 1.82 GPa and 34.3 MPa, respectively (Figures 3M and 3N). The higher tensile strength in DRS straws is due to the removal of aromatic lignin present in RS. ODRS, showed lowered tensile strength and flexural strength of 58 MPa and 2.75 MPa. Upon crosslinking, ODRS_1.6CA showed improvement in flexural and tensile strength to 2.9 MPa and 64 MPa, respectively. On increasing the crosslinking agent concentration, ODRS_3CA displayed enhanced tensile and flexural strength of 66 MPa and 5.9 MPa, respectively (Figures 3J and 3L). Similarly, the tensile modulus of ODRS ~1.67 GPa improved to 2.13 GPa and 2.2 GPa for ODRS_1.6CA and ODRS_3CA straws, respectively. The flexural strength of ODRS showed a value of ~34.5 MPa which improved to 58 MPa and 97 MPa for crosslinked ODRS_1.6CA and ODRS_3CA straws, respectively. The increase in mechanical strength of crosslinked ODRS straws is due to the successful closing of opened sheaths with CA which makes them intact with improved structural stability. Moreover, successful cross-linking of straws led to improved crystallinity along with defect-free closure of open-sheath region as confirmed through XRD, FTIR, and SEM analysis. For flexural strength, ODRS demonstrates comparatively low change in stress with respect to strain beyond 0.02 mm, whereas, upon crosslinking, change in stress with respect to strain improved by three orders of magnitude in the case of ODRS_1.6CA and ODRS_3CA straws. The CA-induced crosslinking of cellulose layers imparts structural strength to ODRS straws; however, it makes the straws slightly brittle in nature. The specific tensile and flexural strength of RS is ~3.5 KNmm/g and 0.082 KNmm/g, respectively, which upon delignification improves to 3.88 KNmm/g and 0.083 KNmm/g (Figures 3O and 3P). The ODRS samples, on the other hand, show lowered specific tensile and flexural strength of 1.77 KNmm/g and 0.083 KNmm/g. On crosslinking, ODRS_1.6CA and ODRS_3CA show improved specific tensile strength of 1.79 KNmm/g and 1.73 KNmm/g and specific flexural strength of ~0.78 KNmm/g and 0.158 KNmm/g, respectively. The developed straws were mechanically strong with tough pointed ends and can be used to directly prick into commercially available packaged fruit juices or beverages (as shown in Video S1), similar to traditional drinking straws. Improvement of overall mechanical strength upon delignification and enhancement of flexural strength in cross-linked ODRS straws, suggests that chemically modified drinking straws from rice crop waste had adequate structural strength making them suitable for beverage consumption.

Evaluation of wettability, water stability, migration properties, antibacterial, and self-cleaning characteristics of straws

The surface-modified and functionalized drinking straws were evaluated for its wettability characteristics by calculating the water contact angle (WCA) change with time. WCA captured as soon as droplet is placed on straws is reported as θ_i and WCA calculated with respect to the diameter of the droplet base is reported as θ_{base}. The change in WCA with time interval was calculated by taking the mean of three sets for every straw with a standard deviation of less than $\pm 5\%$. RS shows initial WCA (θ_i) of ~98.8° which reduced to 76.6° by the end of 20 min, suggesting the inherent hydrophobic nature due to the presence of silica in rice (Figure 4A). The decrease in WCA can be attributed to the spreading of water droplet on the surface of RS. For DRS, a slight enhancement in the WCA values was observed with $\theta_i \sim 105.1°$, which reduced to 81.6° by the end of 20 min. The improvement in hydrophobic properties can be attributed to exposed silica microspheres present on the cellulose surface of DRS, as also observed in SEM micrographs. On crosslinking with CA, ODRS_1.6CA and ODRS_3CA show a reduction in WCA. ODRS_1.6CA initially shows $\theta_i \sim 85.3°$ which reduces to 47.4° whereas ODRS_3CA presents a $\theta_i \sim 87.7°$ which reduces to 51.3° by end of 20 min (Figure 4B). The reduction in θ_i occurs due to the presence of CA at the crosslinked portion which contains hydrophillic carboxyl

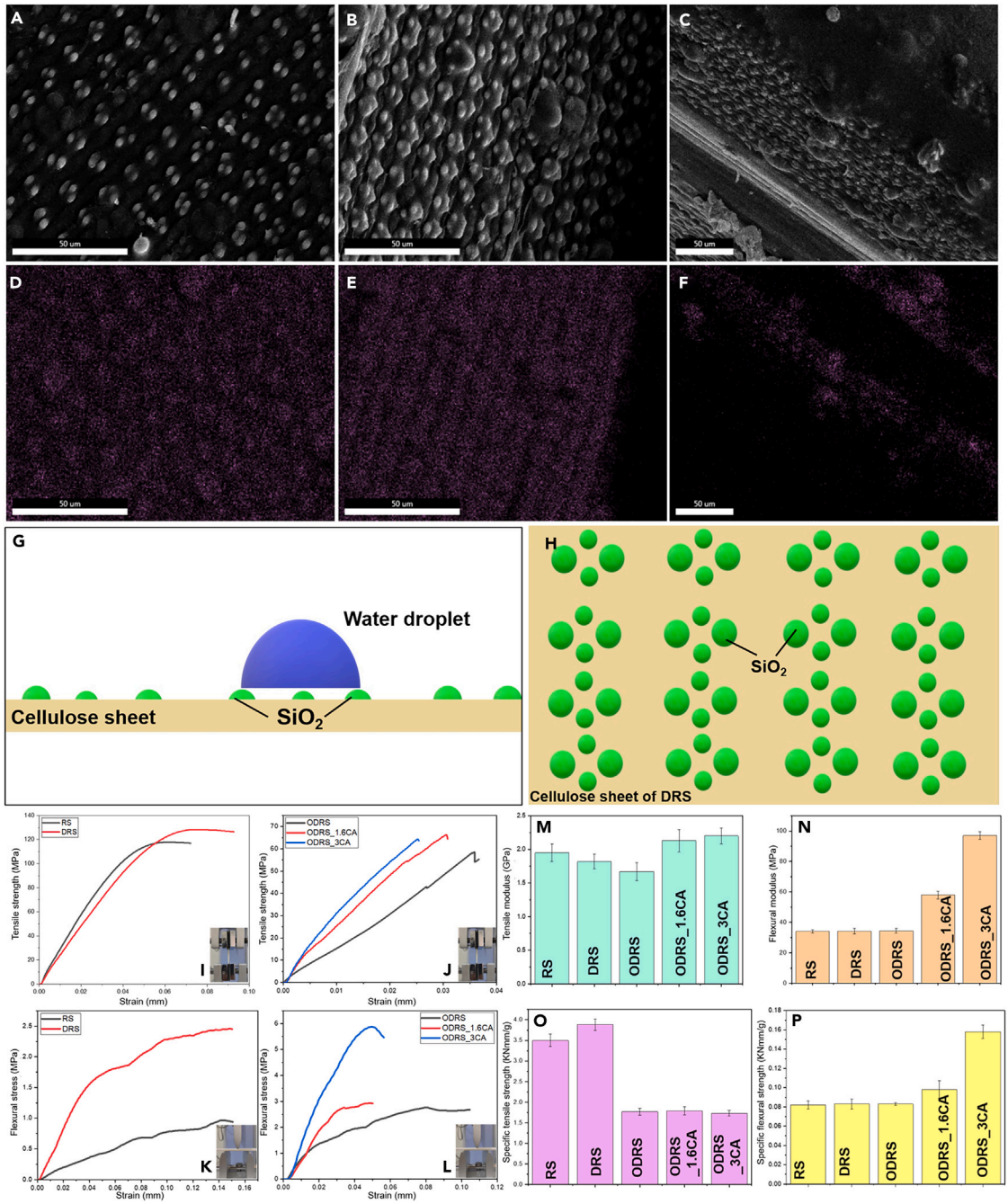

Figure 3. Morphological and mechanical properties of RS, DRS, ODRS_1.6CA, and ODRS_3CA

(A–F) SEM micrographs (scale bar: 50 μm) of (A) RS, (B) DRS, and (C) ODRS_3CA, elemental mapping of silica (Si) in (D) RS (E) DRS, and (F) ODRS_3CA, along with EDX spectrograph (Figure S1).

(G) Water droplet showing hydrophobic characteristics of silica microspheres present on DRS surface preventing its adsorption on cellulose

(H) Schematic representation of the distribution of silica microparticles on DRS.

(I) Tensile strength of RS and DRS.

(J) Tensile strength of ODRS, ODRS_1.6CA, and ODRS_3CA.

(K) Flexural strength of RS and DRS.

(L) Flexural strength of ODRS, ODRS_1.6CA, and ODRS_3CA.

(M) Tensile modulus of RS, DRS, ODRS, ODRS_3CA, and ODRS_1.6CA.

(N) Flexural modulus of RS, DRS, ODRS, ODRS_3CA, and ODRS_1.6CA, also see Video S1.

(O) Specific tensile strength.

(P) Specific flexural strength of RS, DRS, ODRS, ODRS_3CA, and ODRS_1.6CA.

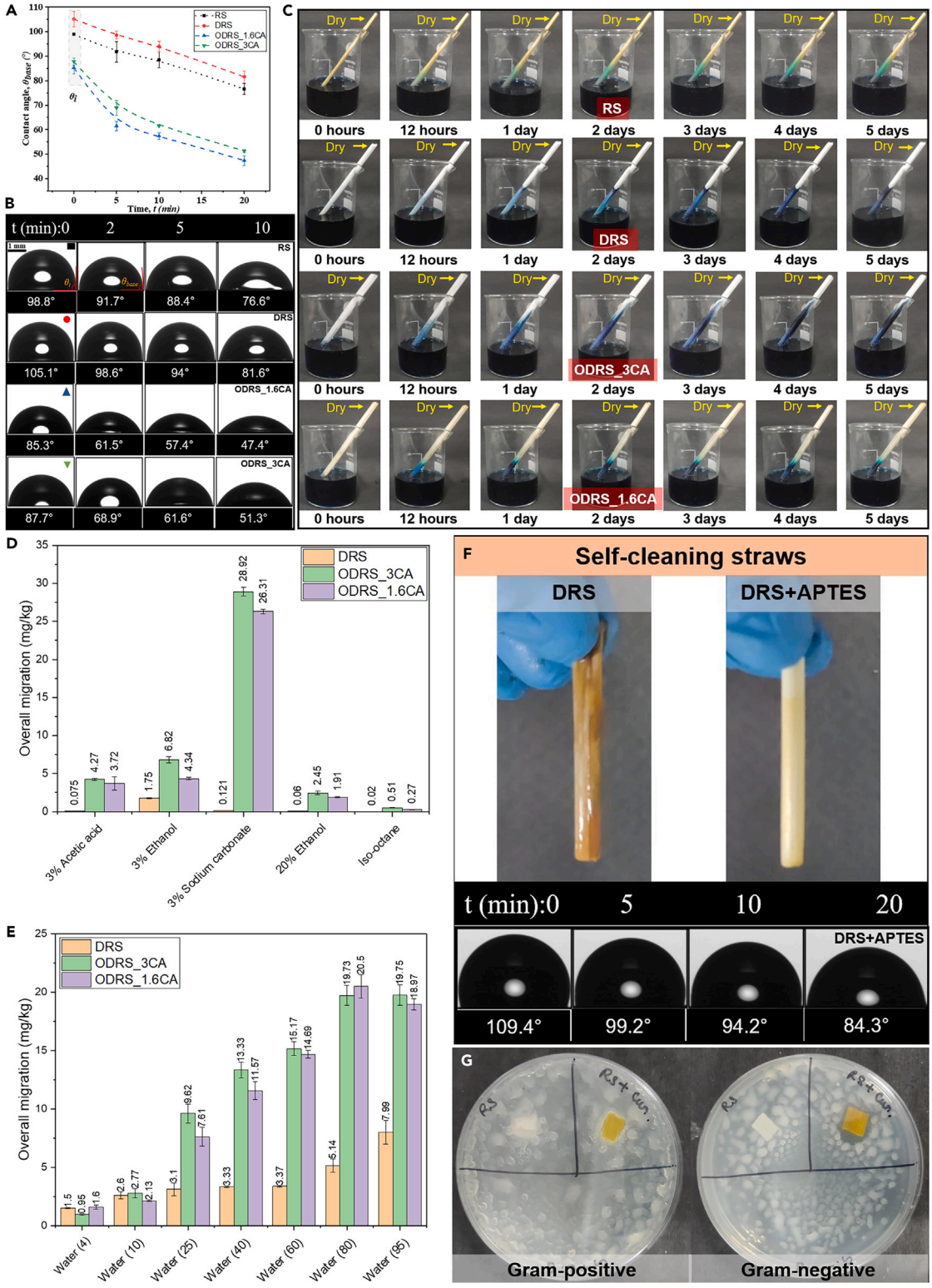

Figure 4. Wettability, water stability, migration properties, antibacterial, and self-cleaning characteristics of straws

(A) Variation in WCA values with time.

(B) Images of WCA variation with time for sessile droplet placed on straws surface (scale bar: 1 mm).

(C) Water stability of RS, DRS, ODRS_1.6CA, and ODRS_3CA straws, solvothermal stability at various temperatures (0°C–95°C) (Figure S2).

Figure 4. *Continued*

(D) Migration values of DRS, ODRS_1.6CA, and ODRS_3CA in acidic, alkaline, alcoholic, carbonated, and fatty beverage.

(E) Migration values of DRS, ODRS_1.6CA, and ODRS_3CA with water at 0°C–95°C.

(F) Demonstration of self-cleaning properties of DRS-APTES straws, also see Figure S3.

(G) Antibacterial activity of DRS-curcumin straws for *S. aureus* (Gram-positive) and *E. coli* (Gram-negative).

groups at the C2 position of its chain. From WCA analysis, it was observed that the presence of silica along with its micro-patterns inherently in RS/DRS straws is responsible for its hydrophobic characteristics which on crosslinking shows reduced wettability but is suitable enough for the drinking straw applications.

Drinking straws are generally used to consume hot or cold beverages; therefore, its stability in the presence of liquid is an important performance parameter.[22] Low-water stability in the presence of beverages is a shortcoming of commercially used paper and bio-based sustainable straw alternatives. For the current work, the water stability of a drinking straw made from RS was evaluated by immersing it in a blue-colored dye solution, and the transport of dye across the straw end was analyzed. All the straw samples i.e., RS, DRS, ODRS_1.6CA, and ODRS_3CA, when immersed for ~5 days in dye solution did not show any wetting at the end (Figure 4C). The blue-colored dye initially travels to the half portion of straws by end of day 1 in almost all straws; however, no significant movement of dye was observed afterward, leaving the other end-of-straw dry. The solvothermal stability of DRS straw was also assessed for temperatures ranging from 0°C to 95°C and it was observed that straws were stable in the entire range of cold-to-hot temperatures (Figure S2). Plant-based lignocellulosic biomass including bamboo and wood usually contains microporous morphology which allows easy travel of water molecules via capillary action. RS on the other hand has a hollow core, with a hydrophobic surface that remains intact even after crosslinking and does not induce any effective capillary forces for the climbing of liquid, resulting in higher water stability. It can be inferred that straws prepared in the current work demonstrate high water stability and do not wet at the non-immersed end of straws even after 5 days which shows its potential in replacing the commercially used soggy paper-based straws and non-degradable plastic straws.

Migration tests were performed to detect the possible leaching of compounds from the straws in the presence of alcoholic, acidic, alkaline, carbonated, and fatty food beverages. For DRS straw, the maximum leaching was observed in the alcoholic beverage simulant (1.75 mg/kg) whereas minimal leaching was observed in the fatty beverage simulant (0.02 mg/kg) (Figure 4D). For ODRS_1.6CA and ODRS_3CA straws, the maximum leaching of 26.31 mg/kg and 28.92 mg/kg were observed in alkaline simulant whereas both straws show minimal leaching in fatty beverages (0.27 mg/kg for ODRS_1.6CA and 0.51 mg/kg for ODRS_3CA). The leaching of components with temperature variation was also studied. For DRS, ODRS_1.6CA, and ODRS_3CA, maximum leaching was observed at 95°C (7.99 mg/kg), 80°C (20.5 mg/kg), and 95°C (19.75 mg/kg), whereas minimum leaching was observed at 4°C (1.5, 1.6, and 0.95 mg/kg) (Figure 4E). The migration studies suggest that DRS, ODRS_1.6CA, and ODRS_3CA straws show very low leaching of components in varied simulants (acidic, alcoholic, alkaline, carbonated, and fatty beverages) and temperature conditions (4°C–95°C). The values for migration were found to be below the standard permitted limits (60 mg/kg), suggesting the possibility of rice waste-based straw application for consuming a wide variety of cold or hot beverages.

The drinking straws prepared in the current study were strategically modified to include antibacterial and self-cleaning properties by incorporating curcumin and silane functionalization, respectively. During APTES modification, the DRS_APTES showed the presence of peaks at 1560 cm^{-1} (N-H bending), 1190 cm^{-1} (Si-O-C stretching), and 1090 cm^{-1} (Si-O-Si stretching) confirming the covalent linking of silane groups with DRS (Figure S3).[31–33] As shown in Figure 4F, the DRS straws on complete immersion in coffee for 10 s result in the retention of brownish-color stain. However, modified DRS-APTES straws do not show any stain on its surface. The DRS-APTES also presents a higher value of $\theta_i \sim$ 109.4° which recedes to 84.3° by the end of 20 min. The silane modifications help in reducing the wettability of straw surfaces which induces self-cleaning characteristics improving their shelf-life and potential reusability. Apart from self-cleaning, the DRS straws were modified with curcumin to introduce antibacterial activity. As shown in Figure 4G, the curcumin-modified DRS straws show strong antibacterial performance against both Gram-positive (left) (*S. aureus*) and Gram-negative (*E. coli*) bacteria (right) with an inhibition zone of 9 mm × 9 mm and 12 mm × 13 mm, respectively. DRS on the other hand, does not present antibacterial activity and allows bacterial growth on its surface. The presence of curcumin was also confirmed with FTIR which showed peaks at 1625 cm^{-1} and 1595 cm^{-1} for C=C stretching and C=O stretching vibration, respectively (Figure S3).[34] The fabrication of antibacterial and self-cleaning rice-based straws opens new avenues to produce cellulose-silica-based adhesive-free smart drinking straws that are safe for consumption.

Self-healing, anti-fizzing, and reusable properties of DRS straws

DRS straws fabricated from rice crop waste were evaluated for its self-healing properties. As shown in Figure 5A, rolled DRS straws were cut vertically to form a sheet, sealed by applying CA (50%), and subsequent crosslinking. The straws were sealed successfully and showed a flexural strength of 1.8 MPa (Figure 5B). The joining of vertically cut DRS is similar to the crosslinking process in ODRS straws; however, a difference would be that leaf sheath portions of ODRS contain opened, rolled overlapped sheets, that are crosslinked by CA. On the other hand, joining a vertical incision does not contain overlapping cellulosic sheets and CA joins the straws side-by-side. To further demonstrate the self-healing of straws, a cut was made in the middle by side and sealed with CA. The straws were perfectly joined after crosslinking (Figure 5C) and showed a flexural strength of 2.5 MPa showing the self-healing of straws for both the vertical and horizontal incisions. The self-healing of DRS straws for vertical and horizontal cuts is mechanistically shown in Figure 5D.

DRS straw was also studied for its anti-fizzing properties, and compared with commercial paper straws. Paper straws due to the presence of a highly heterogenous surface in the form of roughness and uncoated holes, promote effervescence in carbonated beverages as shown in Figure 5E and Video S2.[35] DRS straws, on the other hand, do not form bubbles when immersed in carbonated beverages due to the presence

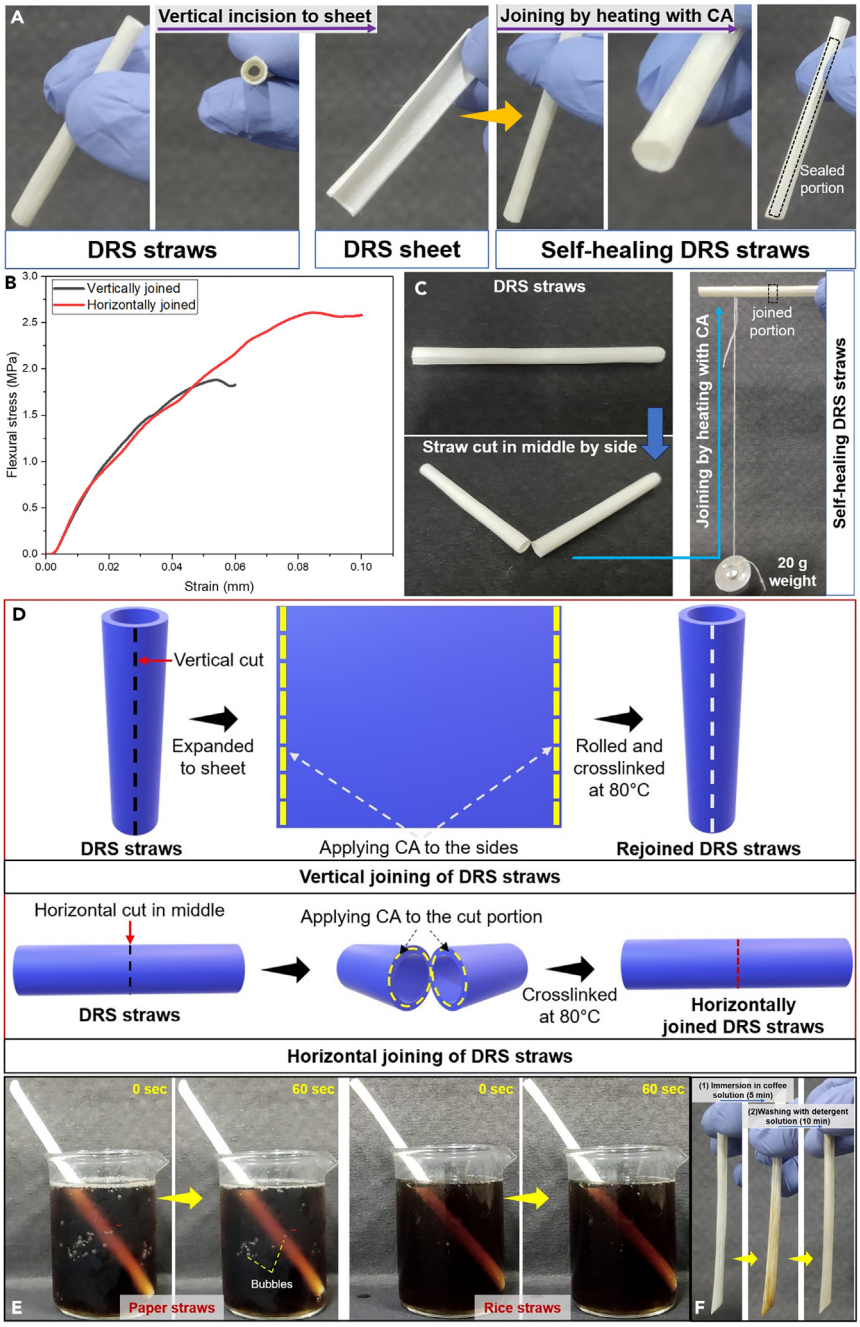

Figure 5. Self-healing, anti-fizzing, and reusable properties of DRS straws

(A) Demonstration of self-healing properties of DRS straws by joining a vertical incision.

(B) Flexural strength of vertically joined and horizontally joined DRS straws.

(C) Self-healing of straws with horizontal cut in middle joined side by side.

(D) Mechanistic representation of joining of vertical and horizontal incision of DRS straws.

(E) Comparison of fizzing properties of paper and RS in carbonated beverage, also see Video S2.

(F) Demonstration of washable and reusable properties of DRS straws by removing a coffee stain from straws with detergent solution.

of uniform surfaces without holes and provide a suitable alternative for the consumption of carbonated beverages. The DRS straws when immersed in a coffee solution get stained with a brown color which was cleaned by putting the straws in a detergent solution indicating that developed straws are washable and can be reused after beverage consumption (Figure 5F). The self-healing, anti-fizzing, and reusable properties of DRS straws make it superior and a potential substitute to the paper straws used currently as the sustainable alternative.

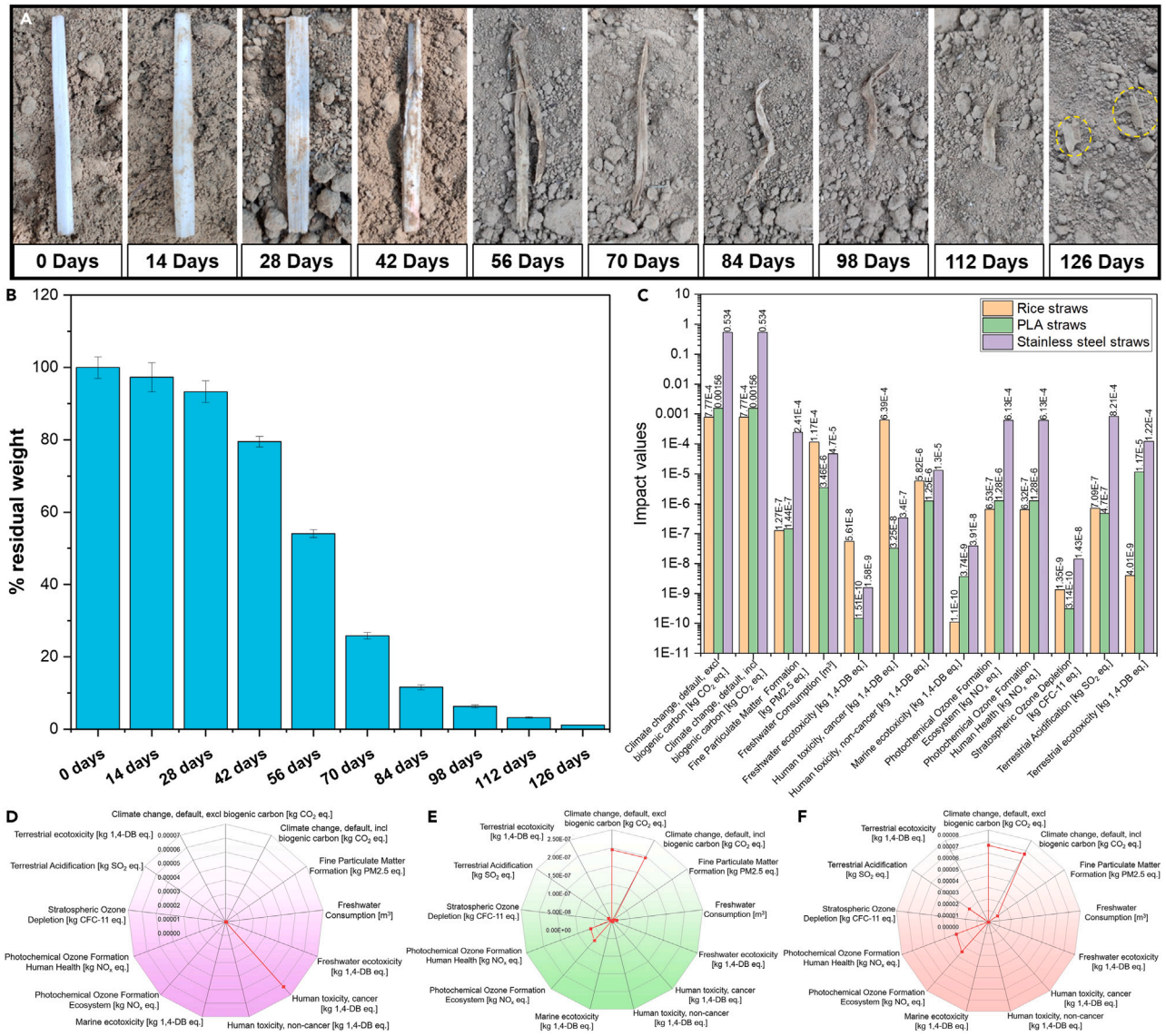

Figure 6. Biodegradation and LCA of rice drinking straws

(A) Changes in the physical appearance of DRS straws during biodegradation studies under garden soil conditions.

(B) Weight loss of straws during biodegradation up to 126 days.

(C) LCA comparison of rice-based ODRS_3CA, stainless steel (SS), and PLA straws.

(D–F) Radar graph for normalized midpoint results of (D) ODRS_3CA, (E) PLA, and (F) SS straws.

Biodegradation and LCA of rice drinking straws

The biodegradation of chemically modified drinking straws from RS was studied under garden soil conditions. For the initial four weeks, only ~6.7% degradation was observed and no significant changes appeared on the surface of straws. However, by the end of eight weeks (56 days), visual change in the physical appearance of straws with initiation of degradation from both ends was observed. Naturally rolled DRS straws degraded into two long pieces, joined only from one end at the end of eight weeks showing a weight loss of ~54.1% (Figures 6A and 6B). Continuing the biodegradation further to twelve weeks resulted in major degradation of straws with the presence of small pieces of DRS which contributed to the remaining weight of ~11.6%. Finally, by the end of 126 days, only small fragments remain with almost ~98.9% degradation suggesting the complete biodegradability of drinking straws prepared using RS.

To evaluate the sustainability associated with the delignification-*cum*-crosslinking based functionalization approach for RS-based drinking straw fabrication, a quantitative analysis of ecological impacts through LCA was conducted and compared with commercially available PLA and stainless steel (SS) straws. For RS drinking straws, the maximum impacts were observed in global warming potential (GWP)/climate change with 0.0007 kg CO_2 eq., human toxicity (0.00063 kg 1,4-DB eq.), and terrestrial acidification (7.09×10^{-7} kg SO_2 eq.) (Figure 6C).

The ecological impacts in GWP category mainly come from the greenhouse gases generated during the cultivation of paddy crops in the oxygen-deficient, anaerobic environment of the field. The lowest ecological impacts were present in marine ecotoxicity of 1.1×10^{-10} kg 1,4-DB eq. followed by terrestrial ecotoxicity (4×10^{-9} kg 1,4-DB eq.) and freshwater ecotoxicity (5.68×10^{-8} kg 1,4-DB eq.). For GWP, PLA straws demonstrate the maximum impact of 0.0015 kg CO_2 eq.; in contrast, SS straws demonstrate 0.534 kg CO_2 eq. For marine and terrestrial ecotoxicity, PLA straws show an impact value of 3.74×10^{-9} kg 1,4-DB eq. and 1.17×10^{-5} kg 1,4-DB, whereas SS straws demonstrate an increased effect to 3.91×10^{-8} kg 1,4-DB, and 1.22×10^{-4} kg 1,4-DB. The high GWP impact for PLA straws comes from the electricity used during polylactide production and straw extrusion whereas for SS straws fuel sources like diesel, natural gas, and electricity were the main contributors. In human toxicity (cancer), human toxicity (non-cancer), and freshwater ecotoxicity category, SS straws show an impact of 3.4×10^{-7}, 1.3×10^{-5}, and 1.51×10^{-10} kg 1,4-DB eq., whereas PLA straws showed an impact of 3.25×10^{-8}, 1.25×10^{-6}, and 3.46×10^{-6} kg 1,4-DB eq. The higher impact of RS on human toxicity and freshwater ecotoxicity comes from rice crop production. SS straws were observed to produce higher impacts in 10 out of 13 categories during cradle-to-gate straw production whereas RS showed a higher impact in the remaining 3 out of 13 categories suggesting that rice-based straws are comparatively more sustainable than SS and PLA straws. Paper and plastic straws as reported in our previous studies generated 0.141 kg CO_2 eq. and 0.005 kg CO_2 eq GWP impact value during cradle-to-gate single straw production which is much higher than RS (0.0007 kg CO_2 eq).[26] In photochemical ozone formation and terrestrial acidification, plastic straws demonstrate the highest impacts, i.e., 2×10^{-4} kg NO_x eq. and 1.72×10^{-4} kg SO_2 eq., followed by paper straws (3.8×10^{-5} kg NO_x eq. for photochemical ozone formation and 2.42×10^{-5} kg SO_2 eq. for terrestrial acidification). RS present minimum impact in both categories with 6.53×10^{-7} kg NO_x eq. for photochemical ozone formation and 7.25×10^{-7} kg SO_2 eq. for terrestrial acidification. Normalization of midpoint results was also carried out to compare the impact categories and select the categories contributing the most ecological effects. Human toxicity (cancer) was observed to be the most dominant category during RS production whereas climate change and photochemical ozone formation were dominant in PLA straw production (Figures 6D and 6E). For SS straws, climate change, photochemical ozone formation, and terrestrial acidification were observed as dominant categories suggesting that SS and PLA straws generate harmful ecological emissions during production, compared to RS (Figure 6F). LCA studies suggest that the strategic chemical modification route used for rice-based drinking straw fabrication in this study generates significantly lower ecological impacts during cradle-to-gate production compared to commercially used paper and plastic straws, providing sustainable alternative straws with interesting physio-chemical and structural properties.

Conclusion

The present study reports a facile, scalable, and low-cost strategy for the up-conversion of rice crop waste into drinking straws infused with self-cleaning, self-healing, anti-fizzing, antibacterial properties, and improved washability for reuse. RS waste (culm and leaf sheath) processed by strategic delignification-*cum*-crosslinking can be utilized to produce biodegradable (~126 days), hydrophobic (WCA ~105.1°), water stable (~5 days), and solvothermal stable (0°C–95°C) drinking straws with high mechanical strength (128 MPa) and flexibility. The outer rolled, opened leaf sheath of RS was cross-linked through the addition of non-toxic, food grade CA which resulted in the fabrication of straws with reduced wettability (87.7°), and high flexural strength (5.9 MPa). All the developed straws show migration values well below the permissible limits (<60 mg/kg) in the presence of different simulants (acidic, alcoholic, alkaline, carbonated, and fatty beverages) at temperature conditions (4°C–95°C). The developed straws also demonstrate lower ecological impacts than SS straws (99.8% less GWP), PLA straws (53.34% less GWP), plastic straws (99.5% less GWP), and paper straws (86% less GWP) suggesting sustainability associated with fabrication strategy used in this study. The curcumin functionalized straws demonstrated antibacterial activity against Gram-positive (*S. aureus*) and Gram-negative bacteria (*E.coli*) with self-cleaning characteristics on strategic silane modification. The proposed scalable route for the valorization of rice wastes to microplastics and adhesive-free drinking straws with multi-functional properties, and lowered ecological impacts provides a sustainable alternative to petroleum-derived single-use non-degradable plastic/paper straws.

Limitations of the study

The separation of RS into culm and leaf sheath has been performed manually in the current work; however, for large-scale production of RS, automated systems are required. The automation experimental research for continuous separation of culm and leaf sheath is undergoing. Another limitation of the work is associated with the reusability of the straws, as it can be reused up to ~5 times only, after which the mechanical stability reduces along with the persistent stain of coffee solutions.

STAR★METHODS

Detailed methods are provided in the online version of this paper and include the following:

- KEY RESOURCES TABLE
- RESOURCE AVAILABILITY
  - Lead contact
  - Materials availability
  - Data and code availability
- METHOD DETAILS
  - Fabrication of delignified and crosslinked drinking straws from rice straws

- Preparation of antibacterial and self-cleaning drinking straws from DRS
- Characterization of rice straws|rice straw-based drinking straws
- Fourier-transform infrared spectroscopy (ATR-FTIR)
- Morphological analysis
- Thermal stability of straws
- Mechanical features of straws
- Water contact angle measurement
- Water stability of drinking straws
- Migration studies for DRS, ODRS_3CA, and ODRS_1.6CA straw
- Antibacterial and self-cleaning activity of drinking straws
- Self-healing, anti-fizzing, and reusable properties of DRS straws
- Biodegradation of DRS straws
- Life cycle analysis of SS, polylactic acid, and ODRS_3CA straws

SUPPLEMENTAL INFORMATION

Supplemental information can be found online at https://doi.org/10.1016/j.isci.2024.109630.

ACKNOWLEDGMENTS

Kant and Ranjan are indebted to Ministry of Education (MOE), Govt. of India (GoI) for the fellowship. Rai would like to acknowledge JRF (junior research fellowship) from Department of Biotechnology (DBT). Dhar is also thankful to DBT for Ramalingaswami fellowship and research project funding (DBTHRDPMU/JRF/BET-20/I/2020/AL/07 and BT/HRD/35/02/2006) for carrying out the research work.

AUTHOR CONTRIBUTIONS

Conceptualization, R.Rai and P.D.; methodology, R.Rai, R.Ranjan, and P.D.; investigation, R.Rai and C.K.; writing – original draft, R.Rai and P.D.; writing – review & editing, R.Rai, R.Ranjan, and P.D.; funding acquisition, P.D.; resources, P.D.; supervision, P.D.

DECLARATION OF INTERESTS

A patent has been submitted for the work reported in this manuscript with patent application no.: 202311061691.

Received: October 26, 2023
Revised: February 5, 2024
Accepted: March 26, 2024
Published: March 28, 2024

REFERENCES

1. FAOSTAT. https://www.fao.org/faostat/en/#data/QCL/visualize.
2. Pathak, H., Singh, R., Bhatia, A., and Jain, N. (2006). Recycling of rice straw to improve wheat yield and soil fertility and reduce atmospheric pollution. Paddy Water Environ. *4*, 111–117. https://doi.org/10.1007/s10333-006-0038-6.
3. Singh, R., Srivastava, M., and Shukla, A. (2016). Environmental sustainability of bioethanol production from rice straw in India: a review. Renew. Sustain. Energy Rev. *54*, 202–216. https://doi.org/10.1016/j.rser.2015.10.005.
4. Liu, Y., Wang, M., Yin, S., Xie, L., Qu, X., Fu, H., Shi, Q., Zhou, F., Xu, F., Tao, S., and Zhu, D. (2022). Comparing Photoactivities of Dissolved Organic Matter Released from Rice Straw-Pyrolyzed Biochar and Composted Rice Straw. Environ. Sci. Technol. *56*, 2803–2815. https://doi.org/10.1021/acs.est.1c08061.
5. Oanh, N.T.K., Bich, T.L., Tipayarom, D., Manadhar, B.R., Prapat, P., Simpson, C.D., and Liu, L.-J.S. (2011). Characterization of particulate matter emission from open burning of rice straw. Atmos. Environ. *45*, 493–502. https://doi.org/10.1016/j.atmosenv.2010.09.023.
6. Namboodiri, M.T., Paul, T., Medisetti, R.M.N., Pakshirajan, K., Narayanasamy, S., and Pugazhenthi, G. (2022). Solid state fermentation of rice straw using Penicillium citrinum for chitosan production and application as nanobiosorbent. Bioresour. Technol. Rep. *18*, 101005. https://doi.org/10.1016/j.biteb.2022.101005.
7. Goto, M., Ehara, H., Karita, S., Takabe, K., Ogawa, N., Yamada, Y., Ogawa, S., Yahaya, M.S., and Morita, O. (2003). Protective effect of silicon on phenolic biosynthesis and ultraviolet spectral stress in rice crop. Plant Sci. *164*, 349–356. https://doi.org/10.1016/S0168-9452(02)00419-3.
8. Wang, S., Wang, N., Yao, K., Fan, Y., Li, W., Han, W., Yin, X., and Chen, D. (2019). Characterization and interpretation of Cd (II) adsorption by different modified rice straws under contrasting conditions. Sci. Rep. *9*, 17868. https://doi.org/10.1038/s41598-019-54337-1.
9. Jin, S., Jin, W., Dong, C., Bai, Y., Jin, D., Hu, Z., and Huang, Y. (2020). Effects of rice straw and rice straw ash on rice growth and α-diversity of bacterial community in rare-earth mining soils. Sci. Rep. *10*, 10331. https://doi.org/10.1038/s41598-020-67160-w.
10. Hakeem, I.Y., Amin, M., Zeyad, A.M., Tayeh, B.A., Maglad, A.M., and Agwa, I.S. (2022). Effects of nano sized sesame stalk and rice straw ashes on high-strength concrete properties. J. Clean. Prod. *370*, 133542. https://doi.org/10.1016/j.jclepro.2022.133542.
11. El-Wahab, R.M.A., Fadel, S.M., Abdel-Karim, A.M., Eloui, S.M., and Hassan, M.L. (2023). Novel green flexible rice straw nanofibers/zinc oxide nanoparticles films with electrical properties. Sci. Rep. *13*, 1927. https://doi.org/10.1038/s41598-023-28999-x.
12. Bilo, F., Pandini, S., Sartore, L., Depero, L.E., Gargiulo, G., Bonassi, A., Federici, S., and Bontempi, E. (2018). A sustainable bioplastic obtained from rice straw. J. Clean. Prod. *200*, 357–368. https://doi.org/10.1016/j.jclepro.2018.07.252.
13. Foong, S.Y., Chan, Y.H., Chin, B.L.F., Lock, S.S.M., Yee, C.Y., Yiin, C.L., Peng, W., and Lam, S.S. (2022). Production of biochar from rice straw and its application for wastewater remediation – An overview. Bioresour.

Technol. *360*, 127588. https://doi.org/10.1016/j.biortech.2022.127588.

14. Kumari, D., and Singh, R. (2022). Rice straw structure changes following green pretreatment with petha wastewater for economically viable bioethanol production. Sci. Rep. *12*, 10443. https://doi.org/10.1038/s41598-022-14627-7.
15. Peng, H., Zhao, W., Liu, J., Liu, P., Yu, H., Deng, J., Yang, Q., Zhang, R., Hu, Z., Liu, S., et al. (2022). Distinct cellulose nanofibrils generated for improved Pickering emulsions and lignocellulose-degradation enzyme secretion coupled with high bioethanol production in natural rice mutants. Green Chem. *24*, 2975–2987. https://doi.org/10.1039/D1GC04447H.
16. Singh, R., and Patel, M. (2022). Effective utilization of rice straw in value-added by-products: A systematic review of state of art and future perspectives. Biomass Bioenergy *159*, 106411. https://doi.org/10.1016/j.biombioe.2022.106411.
17. Geyer, R., Jambeck, J.R., and Law, K.L. (2017). Production, use, and fate of all plastics ever made. Sci. Adv. *3*, e1700782. https://doi.org/10.1126/sciadv.1700782.
18. Luijsterburg, B., and Goossens, H. (2014). Assessment of plastic packaging waste: Material origin, methods, properties. Resour. Conserv. Recycl. *85*, 88–97. https://doi.org/10.1016/j.resconrec.2013.10.010.
19. Li, D., Shi, Y., Yang, L., Xiao, L., Kehoe, D.K., Gun'ko, Y.K., Boland, J.J., and Wang, J.J. (2020). Microplastic release from the degradation of polypropylene feeding bottles during infant formula preparation. Nat. Food *1*, 746–754. https://doi.org/10.1038/s43016-020-00171-y.
20. Vethaak, A.D., and Legler, J. (2021). Microplastics and human health. Science *371*, 672–674. https://doi.org/10.1126/science.abe5041.
21. Chen, C., Wu, Q., Wan, Z., Yang, Q., Xu, Z., Li, D., Jin, Y., and Rojas, O.J. (2022). Mildly processed chitin used in one-component drinking straws and single use materials: Strength, biodegradability and recyclability. Chem. Eng. J. *442*, 136173. https://doi.org/10.1016/j.cej.2022.136173.
22. Yang, H.-B., Liu, Z.-X., Yin, C.-H., Han, Z.-M., Guan, Q.-F., Zhao, Y.-X., Ling, Z.-C., Liu, H.-C., Yang, K.-P., Sun, W.-B., and Yu, S. (2022). Edible, Ultrastrong, and Microplastic-Free Bacterial Cellulose-Based Straws by Biosynthesis. Adv. Funct. Mater. *32*, 2111713. https://doi.org/10.1002/adfm.202111713.
23. Dong, T., Chen, W., Cai, C., Bai, F., Zhou, Z., Wang, J., and Li, X. (2023). Water-stable, strong, biodegradable lignocellulose straws replacement for plastic straws. Chem. Eng. J. *451*, 138970. https://doi.org/10.1016/j.cej.2022.138970.
24. Wang, X., Pang, Z., Chen, C., Xia, Q., Zhou, Y., Jing, S., Wang, R., Ray, U., Gan, W., Li, C., et al. (2020). All-natural, degradable, rolled-up straws based on cellulose micro-and nano-hybrid fibers. Adv. Funct. Mater. *30*, 1910417. https://doi.org/10.1002/adfm.201910417.
25. Wang, X., Xia, Q., Jing, S., Li, C., Chen, Q., Chen, B., Pang, Z., Jiang, B., Gan, W., Chen, G., et al. (2021). Strong, hydrostable, and degradable straws based on cellulose-lignin reinforced composites. Small *17*, 2008011. https://doi.org/10.1002/smll.202008011.
26. Rai, R., Ranjan, R., Kant, C., Ghosh, U.U., and Dhar, P. (2023). Environmentally Benign Partially Delignified and Microwave Processed Bamboo-Based Drinking Straws. Advanced Sustainable Systems *7*, 2300057. https://doi.org/10.1002/adsu.202300057.
27. Rai, R., Ranjan, R., Kant, C., and Dhar, P. (2023). Biodegradable, eco-friendly, and hydrophobic drinking straws based on delignified phosphorylated bamboo-gelatin composites. Chem. Eng. J. *471*, 144047. https://doi.org/10.1016/j.cej.2023.144047.
28. Jin, K., Liu, X., Jiang, Z., Tian, G., Yang, S., Shang, L., and Ma, J. (2019). Delignification kinetics and selectivity in poplar cell wall with acidified sodium chlorite. Ind. Crop. Prod. *136*, 87–92. https://doi.org/10.1016/j.indcrop.2019.04.067.
29. Wang, Y., Yang, Y., Qu, Y., and Zhang, J. (2021). Selective removal of lignin with sodium chlorite to improve the quality and antioxidant activity of xylo-oligosaccharides from lignocellulosic biomass. Bioresour. Technol. *337*, 125506. https://doi.org/10.1016/j.biortech.2021.125506.
30. Siqueira, G., Várnai, A., Ferraz, A., and Milagres, A.M. (2013). Enhancement of cellulose hydrolysis in sugarcane bagasse by the selective removal of lignin with sodium chlorite. Appl. Energy *102*, 399–402. https://doi.org/10.1016/j.apenergy.2012.07.029.
31. Khanjanzadeh, H., Behrooz, R., Bahramifar, N., Gindl-Altmutter, W., Bacher, M., Edler, M., and Griesser, T. (2018). Surface chemical functionalization of cellulose nanocrystals by 3-aminopropyltriethoxysilane. Int. J. Biol. Macromol. *106*, 1288–1296. https://doi.org/10.1016/j.ijbiomac.2017.08.136.
32. Li, X., Wu, Q., Zheng, M., Li, Q., Wang, S., and Zhang, C. (2018). Mechanical, thermal properties and curing kinetics of liquid silicone rubber filled with cellulose nanocrystal. Cellulose *25*, 473–483. https://doi.org/10.1007/s10570-017-1581-6.
33. Shin, J.S., and Oh, T. (2006). Generation of Si-OC bond without Si-CH 3 bond in hybrid type SiOC Film. In 2006 IEEE Nanotechnology Materials and Devices Conference (IEEE), pp. 462–463. https://doi.org/10.1109/NMDC.2006.4388817.
34. Ching, Y.C., Gunathilake, T.M.S.U., Chuah, C.H., Ching, K.Y., Singh, R., and Liou, N.-S. (2019). Curcumin/Tween 20-incorporated cellulose nanoparticles with enhanced curcumin solubility for nano-drug delivery: characterization and in vitro evaluation. Cellulose *26*, 5467–5481. https://doi.org/10.1007/s10570-019-02445-6.
35. Kwak, H., Kim, H., Park, S.-A., Lee, M., Jang, M., Park, S.B., Hwang, S.Y., Kim, H.J., Jeon, H., Koo, J.M., et al. (2022). Biodegradable, Water-Resistant, Anti-Fizzing, Polyester Nanocellulose Composite Paper Straws. Adv. Sci. *10*, 2205554. https://doi.org/10.1002/advs.202205554.
36. Fu, Q., Ansari, F., Zhou, Q., and Berglund, L.A. (2018). Wood nanotechnology for strong, mesoporous, and hydrophobic biocomposites for selective separation of oil/water mixtures. ACS Nano *12*, 2222–2230. https://doi.org/10.1021/acsnano.8b00005.
37. Neves, R.M., Ornaghi, H.L., Jr., Zattera, A.J., and Amico, S.C. (2020). The influence of silane surface modification on microcrystalline cellulose characteristics. Carbohydr. Polym. *230*, 115595. https://doi.org/10.1016/j.carbpol.2019.115595.
38. Chang, L., and Tan, J. (2021). An integrated sustainability assessment of drinking straws. J. Environ. Chem. Eng. *9*, 105527. https://doi.org/10.1016/j.jece.2021.105527.

STAR★METHODS

KEY RESOURCES TABLE

REAGENT or RESOURCE	SOURCE	IDENTIFIER
Chemicals, peptides, and recombinant proteins		
Ethanol	Merck Millipore	CAS: 64-17-5
Sodium chlorite	HiMedia Laboratories Pvt. Ltd.	CAS: 7758-19-2
Agar	HiMedia Laboratories Pvt. Ltd.	CAS: 9002-18-0
Acetic acid	Sisco Research Laboratories Pvt. Ltd.	CAS: 64-19-7
Sodium acetate	Sisco Research Laboratories Pvt. Ltd.	CAS: 127-09-3
Citric acid	Sisco Research Laboratories Pvt. Ltd.	CAS: 5949-29-1
Curcumin	Sisco Research Laboratories Pvt. Ltd.	CAS: 458-37-7
(3-Aminopropyl)triethoxysilane	Sisco Research Laboratories Pvt. Ltd.	CAS: 919-30-2
Sodium carbonate	Sisco Research Laboratories Pvt. Ltd.	CAS: 497-19-8
Isooctane	Sisco Research Laboratories Pvt. Ltd.	CAS: 540-84-1
Nutrient broth	Sisco Research Laboratories Pvt. Ltd.	Product code: 55427
Rice straw	Agricultural site of the Institute of Agricultural Sciences, Banaras Hindu University (BHU), Varanasi, India	
Deposited data		
Stainless steel production	Chang, L., and Tan, J. (2021). An integrated sustainability assessment of drinking straws. Journal of Environmental Chemical Engineering 9, 105527.[38]	https://doi.org/10.1016/j.jece.2021.105527
Other		
ecoinvent database V3.9	ecoinvent	https://ecoinvent.org/
GaBi education database (2020)	Sphera Solutions, Inc.	https://sphera.com/life-cycle-assessment-lca-software/

RESOURCE AVAILABILITY

Lead contact

Further information and requests for resources should be directed to the lead contact, Prodyut Dhar (prodyut.bce@iitbhu.ac.in).

Materials availability

The study did not generate new unique materials.

Data and code availability

- Data reported in this paper will be shared by the lead contact upon reasonable request.
- This study does not report any original code.
- Any additional information required to reanalyze the data reported in this paper is available from the lead contact upon reasonable request.

METHOD DETAILS

Fabrication of delignified and crosslinked drinking straws from rice straws

Dried RS were cut between nodes from the plant base with a length of 9 cm which were opened and the rolled leaf sheath portion was separated from closed stem culms (as shown in Figure 1). Delignification was performed by immersing 5g of RS in 0.5% sodium chlorite (50 mL) prepared in acetate buffer with pH~4.6 at 80°C for 8 h.[36] For the preparation of sodium acetate buffer, sodium acetate (5.4 g) and acetic acid (2.4 g) were mixed with ultrapure water (~0.66 mΩ/cm conductivity) to prepare 100 mL of acetate buffer, followed by adjusting the pH to ~4.6. After delignification, delignified closed RS culms (denoted as DRS) and opened delignified leaf sheath of RS (denoted as ODRS) were washed until the unreacted chemicals were removed and dried at 25°C for 12 h. The dried ODRS (5g) were closed by immersing straws in 50% and 40%

CA (50 mL) for 4 h, followed by heat-induced crosslinking at 80°C for 30 min. Crosslinked ODRS were then washed to remove unreacted CA, and air dried for 12 h at room temperature (25°C), to produce ODRS_3CA [ODRS (immersed in 50% CA) containing 3% CA by weight after washing], and ODRS_1.6 CA [ODRS (immersed in 40% CA)] containing 1.6% CA after washing.

Preparation of antibacterial and self-cleaning drinking straws from DRS

For preparing antibacterial straws, dried DRS straws were immersed in 50 mL of 3 mg/mL curcumin dissolved in dimethyl sulfoxide (DMSO) for 8 h at 25°C, and washed with ultrapure water multiple times to remove the unbounded curcumin present on the surface of the straw, followed by freeze drying for 8 h. For the preparation of self-cleaning straws, silane modification of DRS using APTES was done as per earlier report by Neves et al.[37] with slight modifications. Briefly, DRS was immersed in 75:25 (v/v) ethanol: water solution acidified to pH 4–5 for 30 min. APTES was then hydrolyzed in ethanol: water solution using acetic acid and stirred for 30 min. Subsequently, DRS straws were immersed in hydrolyzed APTES solution and kept at stirring for 2 h. Afterward, DRS was cured at 105°C for 15 min and washed using ultrapure water several times to remove unreacted APTES, followed by drying at room temperature.

Characterization of rice straws|rice straw-based drinking straws

X-Ray diffraction

For XRD analysis, samples were scanned in the range of $2\theta \sim 5$–60° at scan rate of 5°/min and step size of 0.01° using Bench-Top XRD (MiniFlex600, Rigaku). Dried straw samples were spread over the sample holder and CuK_{α} anode (k = 1.54 Å) was used to generate radiation from copper anticathode with a current of 20-mA and emission voltage of 40 kV. The percent crystallinity (% crystallinity), and crystallinity index (*CI*), were calculated as per the Segal equation:

$$CI = \frac{I_{002} - I_{am}}{I_{002}} \quad \text{(Equation 1)}$$

where I_{002} denotes crystalline diffraction peak intensity and I_{am} is amorphous peak intensity.

Fourier-transform infrared spectroscopy (ATR-FTIR)

FTIR analysis was carried out in transmittance mode from 650 to 4000 cm^{-1} wavelength using ZnSe crystal, with a resolution of 4 cm^{-1} and 64 scans on Agilent Cary 630 FTIR, Malaysia, and the data was collected by Microlab software (Agilent, Malaysia). The samples were pressed using a swivel press onto the ATR crystal for proper contact between the crystal and the sample's surface.

X-ray photoelectron spectroscopy (XPS)

XPS of RS, and ODRS_3CA was conducted using Thermo Scientific K-alpha (US). The sample was mounded over the holder that goes to the analysis chamber. 0.1 and 1 eV step sizes were used for narrow and survey scanning, respectively. Analysis was conducted under vacuum (10^{-8}–10^{-9} mbar) using AlKα anode, a 400 µm beam spot size, and a binding energy of −10–1350 eV

Morphological analysis

The dried straw samples were cut vertically to form sheets using a doctor blade for scanning electron microscopy (SEM) analysis (Nova Nano SEM 450, FEI, USA), at an accelerating voltage of 10 kV. Gold and palladium foil-based double coating was performed on samples using DSR1(UK) desk sputter coater at 200 Torr pressure for ∼180 s. EDX (EDAX, USA) was used to analyze the elements present on the sample surfaces (at an accelerated voltage of 10 kV) and mapped using Team Basic software.

Thermal stability of straws

Thermal properties of straw samples were analyzed with PerkinElmer STA6000 (USA). Samples were put in a platinum crucible and thermally degraded by heating from 25°C to 700 °C at 10 °C/min heating rate. The test was carried out under inert conditions in the presence of nitrogen gas flowing at 10 mL/min to measure the variation in gravimetric signals.

Mechanical features of straws

The mechanical properties of straws were calculated using texture analyzer EZ-SX, EZ-Test, Shimadzu, Japan, equipped with 500 N load cell at a uniform speed of 1 mm/s. Straws with a diameter of 4 mm and length of 5 cm were used for tensile and flexural tests, and mean observations for at least three samples were reported. The specific tensile and specific flexural strength was calculated using Equations 2 and 3:

$$\text{Specific tensile strength} = \frac{\text{Tensile strength (maximum) (MPa)}}{\text{Density (g/mm3)}} \quad \text{(Equation 2)}$$

$$\text{Specific flexural strength} = \frac{\text{Flexural strength (maximum) (MPa)}}{\text{Density (g/mm3)}} \quad \text{(Equation 3)}$$

Water contact angle measurement

Sessile water droplets of 5 μL volume were put at the surface of straws to measure the WCA using Theta Lite, Biolin Scientific (Sweden). The change in WCA with time was calculated by recording video at 5 frames per second at 25°C. The WCA was calculated with OneAttension software (Biolin Scientific, Sweden), and the observation of atleast three samples was used to report the average values.

Water stability of drinking straws

Water stability is a crucial parameter for drinking straws, for which the straws were immersed partially in 20 mL blue-colored solution (10 mg/ml, food-grade dye) at 25°C. To study solvothermal stability at varied temperatures, straws were partially immersed in the dye solution and kept at 0, 10, 40, 60, 80, and 95°C temperatures. The movement of dye color across the length of straws was observed at the circumference and end-tip to track the water transport.

Migration studies for DRS, ODRS_3CA, and ODRS_1.6CA straw

Straws used for drinking applications come in contact with food directly, therefore, migration studies to analyze the leaching of non-edible and edible components were carried out as it can impact the beverage quality and user experience. The straws were analyzed for migration of components using acetic acid (3%) (acidic simulant), sodium carbonate (3%) (alkaline simulant), ethanol (3%) (alcoholic simulant), ethanol (20%) (carbonated simulant), and isooctane (fatty simulant). Experiments were carried out following Commission Regulation EU No.10/2011 with some modifications.[27] Straws (9 cm) were completely immersed in a glass tube containing 40 mL of simulant for 24 h and closed with paraffin tightly to minimize the loss of simulants. The migration of components at different temperatures (4, 10, 25, 40, 60, 80, and 95°C) was also analyzed by immersing the straws in ultrapure water for 24 h. After the migration studies, tubes containing simulants were dried at 105°C and observed for weight change. Migration values were calculated in mg/kg for at least three different triplicate straws using Sartorius QUINTIX65, Germany (+0.01 mg precision) analytical balance.

Antibacterial and self-cleaning activity of drinking straws

For the estimation of antibacterial properties against gram-negative and gram-positive bacteria, fresh cultures of *Staphylococcus aureus* and *Escherichia coli* were inoculated in nutrient broth and incubated for 16 h. The growth in the culture tubes was confirmed by turbidity change, which was then plated to nutrient agar (100 μL). After 30 min of incubation of agar plates at 37°C, a sheet (1 cm × 1 cm) was cut from DRS and DRS-curcumin (DRS-cur) straws and placed on the inoculated nutrient agar plates. Incubation was done overnight and the bacterial growth inhibition zone was measured to confirm the antibacterial activity. For assessment of self-cleaning properties of straws, both DRS and APTES modified DRS straws (DRS-APTES) were immersed in hot coffee (80°C) for 5 s and observed for retention of any coffee stain on its surface.

Self-healing, anti-fizzing, and reusable properties of DRS straws

To assess the self-healing properties, a vertical cut was made to DRS straws (~5 cm) to form a sheet, and a horizontal cut was made in the middle of straws (~10 cm) by side. The straws were rejoined by applying CA (50%) to both sides and ends of cut straws and kept at 80°C for 2 h. After crosslinking, extra CA was removed by washing with distilled water and drying at room temperature (25°C).

For anti-fizzing properties, straws were immersed in carbonated beverages (40 mL) and observed for the formation of fizz or bubbles for a period of ~10 min, and video was recorded.

The reusability of DRS straws was assessed by immersing the straws in a coffee solution for 5 min, followed by immersion in a detergent solution to remove the coffee stain for 10 min. The straws were air-dried at room temperature (25°C) to evaluate the removal of stains.

Biodegradation of DRS straws

The straws were placed at ~4 cm depth, below the garden soil surface to carry out the biodegradation studies. The degraded straws were taken out at different time intervals (days) to calculate the weight change and determine the %biodegradation according to Equation 4:

$$\text{Biodegradation (\%)} = \frac{W1 - W2}{W1} \times 100 \quad \text{(Equation 4)}$$

where w_1 and w_2 present the initial weight and final weight of degraded straws, respectively.

Life cycle analysis of SS, polylactic acid, and ODRS_3CA straws

LCA was conducted to quantify the ecological impacts generated during the production of drinking straws using rice crop waste following delignification-*cum*-cross-linking strategy. The system boundary of the study involves cradle-to-gate approach with the processing of rice biomass for the preparation of drinking straws by utilizing chemicals and energy as inputs (Figure S4). For ODRS_3CA,

the straw-making steps are rice crop production, delignification of RS, and subsequent crosslinking (Figure S5). For comparison with sustainable and reusable straw alternatives commercially available in the market such as PLA and SS straws. The cradle-to-gate life cycle of PLA straws involves polylactide production followed by extrusion to produce straws (Figure S6). For SS straws, the steps involved the production of SS sheets using chromium, iron, and nickel and its processing by heating, welding, extrusion, and casting for the fabrication of straws (Figure S7).[38] One straw was taken as a functional unit, and ReCiPe (H) method (ReCiPe 2016 v1.1) was used for ecological impact calculation in the current work. The LCA was conducted in GaBi(version 9.2.1.68), and electricity derived from natural gas was used for calculations.